

Supplementary Material

Supplementary Table 1: MAIT tissue repair genes also upregulated by bronchoalveolar MAIT cells in comparison to peripheral blood MAIT cells.

Gene	Log ₂ Fold Change	Adjusted P
<i>IL1B</i>	5.4659	0.0119
<i>CXCL10</i>	5.3120	0.0871
<i>JAG2</i>	4.6732	0.0926
<i>PMP22</i>	4.4515	0.0644
<i>CXCL2</i>	4.4232	0.0616
<i>TNFRSF21</i>	4.0764	0.0918
<i>CSF2</i>	4.0119	0.1972
<i>HBEGF</i>	3.9078	0.1008
<i>INHBA</i>	3.8365	0.2714
<i>FLG</i>	3.5022	0.2018
<i>APOE</i>	3.3867	0.2262
<i>WNT10A</i>	3.1996	0.2962
<i>ADM</i>	2.7396	0.5015
<i>ZBTB7C</i>	2.3640	0.4231
<i>ENG</i>	2.0479	0.1762
<i>LGALS3</i>	2.0072	0.0746
<i>ADAMTS2</i>	1.7944	0.2769
<i>SYK</i>	1.7857	0.1743
<i>CXCL12</i>	1.5037	0.6055
<i>IGF1</i>	1.2513	0.1127
<i>CSF1R</i>	1.2232	0.6028
<i>PDGFA</i>	1.0010	0.6487
<i>THBS1</i>	0.9028	0.5151
<i>FGFR2</i>	0.8919	0.2309
<i>CSF1</i>	0.7786	0.5034
<i>CCL3</i>	0.7190	0.6362
<i>BMP7</i>	0.6525	0.3417
<i>DISP1</i>	0.5697	0.7446
<i>EREG</i>	0.5116	0.5041
<i>FLG2</i>	0.4911	0.6169
<i>LEP</i>	0.4810	0.7144
<i>EPGN</i>	0.4482	0.5569
<i>WNT7B</i>	0.3903	0.6004
<i>APP</i>	0.3797	0.8234
<i>ANGPT2</i>	0.2230	0.7109
<i>CRISPLD2</i>	0.1924	0.8829

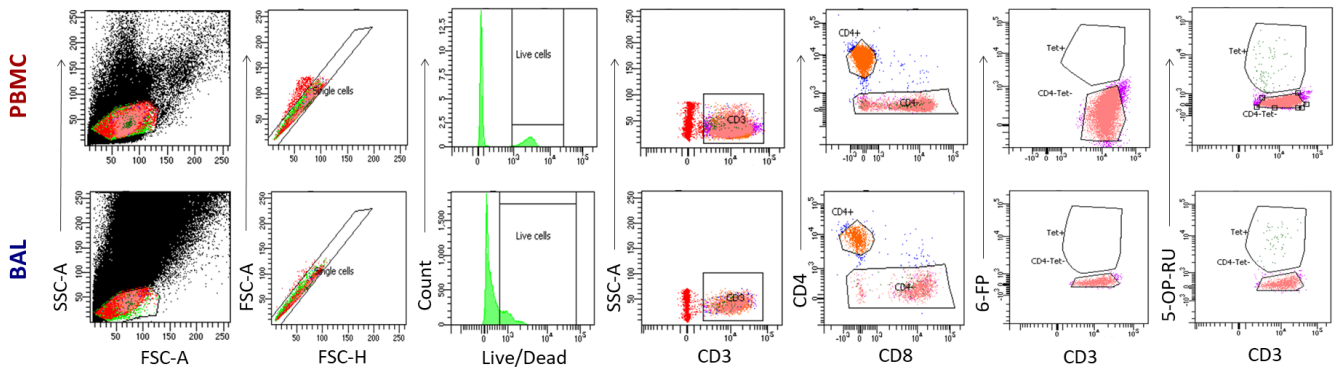
<i>HIF1A</i>	0.1474	0.9027
<i>IFT172</i>	0.0849	0.9665
<i>VEGFB</i>	0.0816	0.9475

Supplementary Table 2: Genes differentially expressed by MR1 tetramer-negative TRAV1-2+CD161+CD8+ T cells cells during latent TB infection and similarly differentially expressed by bronchoalveolar MAIT cells as compared to peripheral blood MAIT cells.

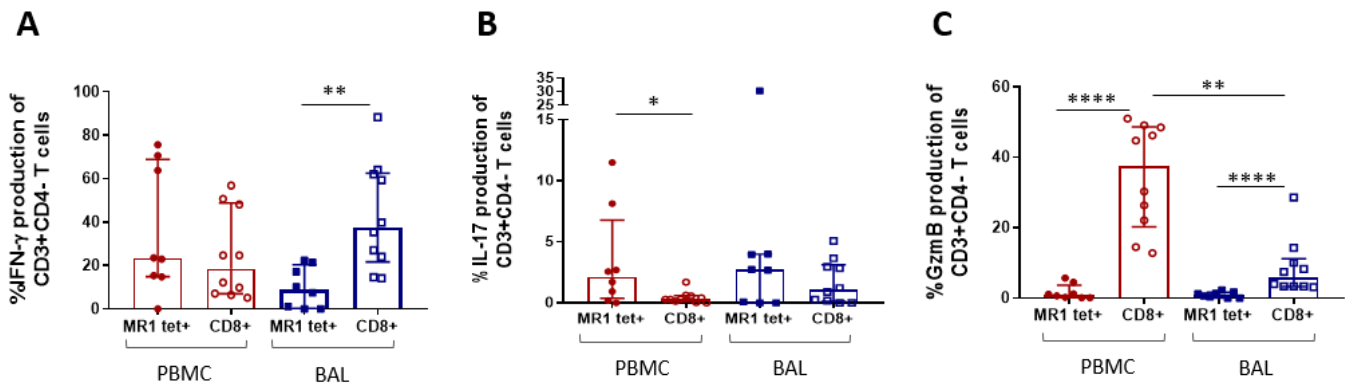
Downregulated genes			Upregulated genes		
Gene	Log ₂ Fold Change	Adjusted P	Gene	Log ₂ Fold Change	Adjusted P
<i>SHQ1</i>	-2.6701	0.0284	<i>CD4</i>	4.2899	0.0694
<i>UCHL5</i>	-2.1101	0.0491	<i>MYLK4</i>	3.0350	0.0921
<i>DCP1B</i>	-1.7564	0.1866	<i>TNFAIP2</i>	2.7483	0.2181
<i>KIAA0922</i>	-1.3915	0.2070	<i>CST3</i>	2.5643	0.2736
<i>GOT2</i>	-1.3571	0.2150	<i>HLA-DRB6</i>	2.5482	0.0698
<i>CLPTM1</i>	-1.3420	0.1664	<i>PTAFR</i>	2.5395	0.0009
<i>REXO4</i>	-1.3369	0.2481	<i>SYK</i>	1.7857	0.1743
<i>DUS2L</i>	-1.2888	0.4092	<i>EMR2</i>	1.7575	0.1492
<i>DYM</i>	-1.2671	0.2520	<i>DYDC1</i>	1.6938	0.1745
<i>UAPI</i>	-1.2588	0.2778	<i>LOC148709</i>	1.6510	0.2260
<i>ADK</i>	-1.2569	0.2680	<i>UCKL1-AS1</i>	1.2333	0.1327
<i>SF3B4</i>	-1.2379	0.2404	<i>FFAR2</i>	1.2208	0.1693
<i>G6PD</i>	-1.1753	0.2812	<i>TMEM170B</i>	1.1443	0.1714
<i>SUCLG2</i>	-1.1519	0.3105	<i>LOC284379</i>	1.1325	0.1008
<i>TBC1D14</i>	-1.0872	0.3873	<i>POU5F1</i>	1.1270	0.1433
<i>EHMT1</i>	-1.0569	0.2885	<i>PARD6G</i>	1.1220	0.0832
<i>C17orf62</i>	-1.0178	0.3102	<i>C4orf26</i>	1.1031	0.1397
<i>DDB1</i>	-1.0110	0.3546	<i>INMT</i>	1.0740	0.1059
<i>PSMC4</i>	-0.9982	0.3227	<i>NLRP12</i>	1.0387	0.1513
<i>MDH2</i>	-0.9210	0.3924	<i>ITGA2</i>	1.0100	0.2177
<i>FNTA</i>	-0.8901	0.4044	<i>SLC16A12</i>	0.9879	0.3541
<i>NFYB</i>	-0.8863	0.3046	<i>LOC100506385</i>	0.9696	0.2255
<i>P4HTM</i>	-0.8772	0.4338	<i>CNNM1</i>	0.9499	0.2671
<i>SAE1</i>	-0.8015	0.4571	<i>BHMT2</i>	0.9432	0.1588
<i>RHBDD2</i>	-0.7844	0.4511	<i>MBOAT2</i>	0.9405	0.2610
<i>PSMC2</i>	-0.7532	0.4045	<i>NDST3</i>	0.8965	0.2561
<i>DENND2D</i>	-0.6513	0.5297	<i>C9orf66</i>	0.8714	0.2814
<i>KCNA3</i>	-0.6052	0.5338	<i>IL17RD</i>	0.8516	0.2422
<i>CASP8</i>	-0.5869	0.2509	<i>GSTTP2</i>	0.8512	0.3037

<i>AP3S2</i>	-0.5843	0.4798	<i>FBLIM1</i>	0.8419	0.1897
<i>KDELR2</i>	-0.5626	0.5786	<i>LOC100292680</i>	0.8375	0.5657
<i>YTHDF2</i>	-0.5545	0.5784	<i>FOXP4</i>	0.8366	0.2492
<i>ARCN1</i>	-0.4939	0.4761	<i>ADCY1</i>	0.8257	0.3401
<i>ATF2</i>	-0.4807	0.6711	<i>PART1</i>	0.8200	0.2501
<i>HADHB</i>	-0.4558	0.6642	<i>EMX2OS</i>	0.8016	0.2076
<i>SSR1</i>	-0.3165	0.4241	<i>TMEM17</i>	0.7826	0.3050
<i>CCR1</i>	-0.3157	0.8277	<i>IAPP</i>	0.7728	0.2636
<i>ACTR3</i>	-0.1953	0.8609	<i>C21orf62</i>	0.7703	0.1990
<i>ACAD11</i>	-0.1938	0.8798	<i>LOC100129269</i>	0.7659	0.2206
<i>CNDP2</i>	-0.1604	0.8786	<i>SIPR3</i>	0.7407	0.4457
<i>PTPN22</i>	-0.1474	0.8947	<i>C14orf105</i>	0.7352	0.3690
-	-	-	<i>RAB3B</i>	0.7261	0.2027
-	-	-	<i>PTK6</i>	0.7249	0.2904
-	-	-	<i>MSRB3</i>	0.7112	0.2961
-	-	-	<i>C1orf140</i>	0.7106	0.3481
-	-	-	<i>LOC100128338</i>	0.7095	0.2399
-	-	-	<i>FRRS1</i>	0.7081	0.3074
-	-	-	<i>ST6GAL2</i>	0.7039	0.3916
-	-	-	<i>FCAR</i>	0.7026	0.2764
-	-	-	<i>PSME4</i>	0.6888	0.4503
-	-	-	<i>AGMO</i>	0.6763	0.4114
-	-	-	<i>OLFML2A</i>	0.6762	0.2584
-	-	-	<i>CEACAM8</i>	0.6610	0.4789
-	-	-	<i>KREMEN1</i>	0.6568	0.2485
-	-	-	<i>LOC100287792</i>	0.6423	0.2394
-	-	-	<i>SYNPO2</i>	0.6343	0.3566
-	-	-	<i>LAMC2</i>	0.6269	0.5295
-	-	-	<i>TLCD2</i>	0.5985	0.2482
-	-	-	<i>CABP4</i>	0.5924	0.2043
-	-	-	<i>IRGQ</i>	0.5852	0.1588
-	-	-	<i>TTL</i>	0.5747	0.6595
-	-	-	<i>VSTM4</i>	0.5738	0.3236
-	-	-	<i>TRIM58</i>	0.5723	0.2671
-	-	-	<i>PDE6A</i>	0.5612	0.3774
-	-	-	<i>LOC100128682</i>	0.5426	0.2764
-	-	-	<i>LOC729603</i>	0.5388	0.3410
-	-	-	<i>CACNG8</i>	0.5231	0.2724
-	-	-	<i>EMP2</i>	0.5182	0.3263
-	-	-	<i>CEACAM22P</i>	0.4735	0.3803
-	-	-	<i>MYLK3</i>	0.4354	0.3615
-	-	-	<i>FLJ43879</i>	0.4261	0.4326
-	-	-	<i>LOC284950</i>	0.4236	0.4711
-	-	-	<i>CHST6</i>	0.3997	0.4104
-	-	-	<i>SLC36A2</i>	0.3795	0.5738
-	-	-	<i>POM121L10P</i>	0.3724	0.4466

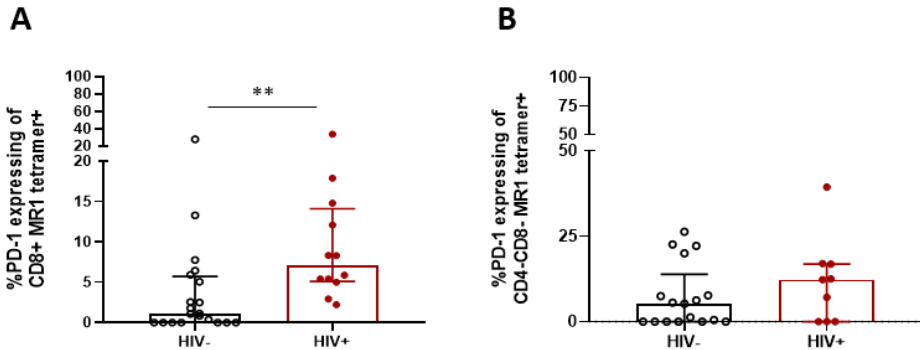
-	-	-	<i>LOC100128288</i>	0.3585	0.5745
-	-	-	<i>KLB</i>	0.3401	0.5633
-	-	-	<i>NWD1</i>	0.3397	0.5703
-	-	-	<i>SLC15A2</i>	0.2983	0.6820
-	-	-	<i>FKBP9</i>	0.2884	0.6537
-	-	-	<i>ARGFX</i>	0.2784	0.4804
-	-	-	<i>CPA4</i>	0.2259	0.7484
-	-	-	<i>NAPSB</i>	0.2116	0.9262
-	-	-	<i>TSIX</i>	0.2041	0.7849
-	-	-	<i>ARSD</i>	0.1710	0.8481
-	-	-	<i>C3orf62</i>	0.1082	0.8512
-	-	-	<i>LOC400548</i>	0.0885	0.9055
-	-	-	<i>FHDC1</i>	0.0711	0.9386
-	-	-	<i>LOC286437</i>	0.0688	0.9345
-	-	-	<i>AFF3</i>	0.0464	0.9434
-	-	-	<i>S100PBP</i>	0.0087	0.9931



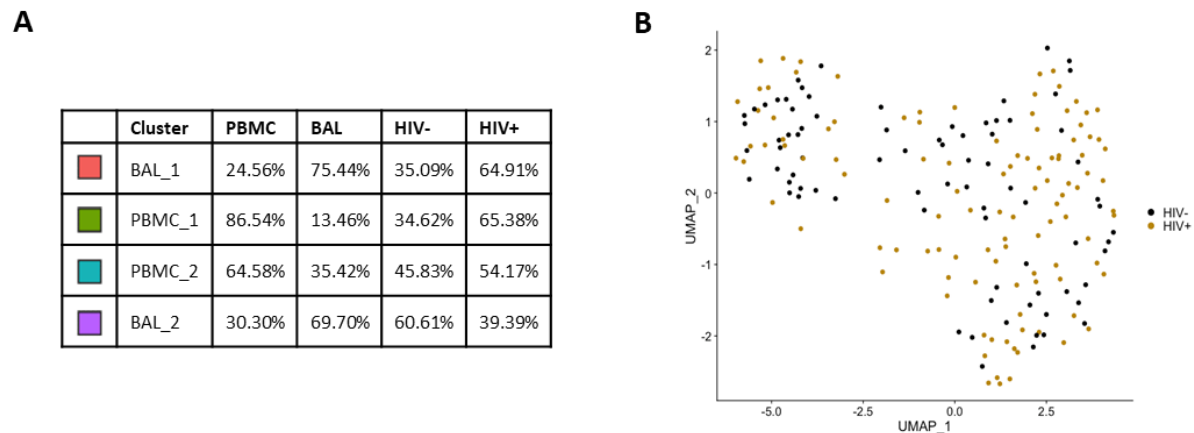
Supplementary Figure 1: Gating strategy used to sort MR1 tetramer-positive MAIT cells for RNA-sequencing. Cells were sorted from the peripheral blood and bronchoalveolar compartments using the MR1 6-FP tetramer to define the MR1 5-OP-RU tetramer gate.



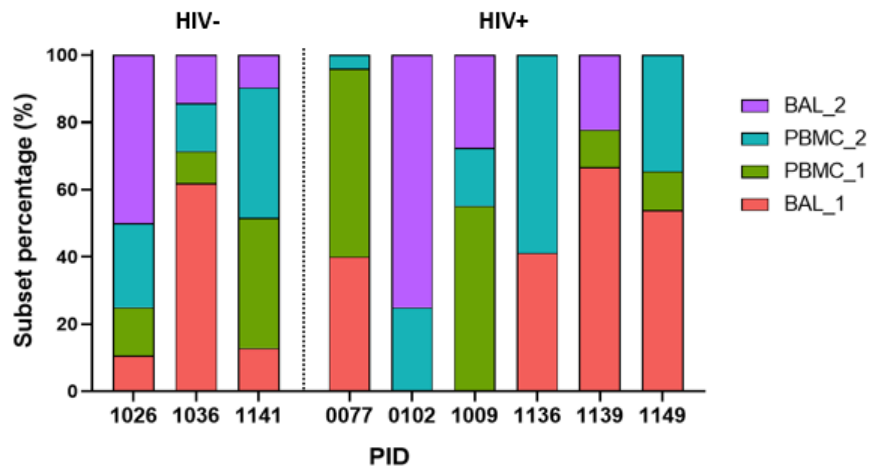
Supplementary Figure 2: Pro-inflammatory cytokine and cytolytic molecule production of MR1 tetramer-positive MAIT cells ($n = 8$) in the peripheral blood (red) and bronchoalveolar lavage (BAL) fluid (blue) in contrast to matched conventional CD8+ T cells ($n = 10$) from healthy participants showing (A) inducible IFN- γ , (B) inducible IL-17 and (C) constitutive granzyme B production. Bars represent medians and error bars represent interquartile ranges. Statistical difference was determined using the Mann-Whitney U test.



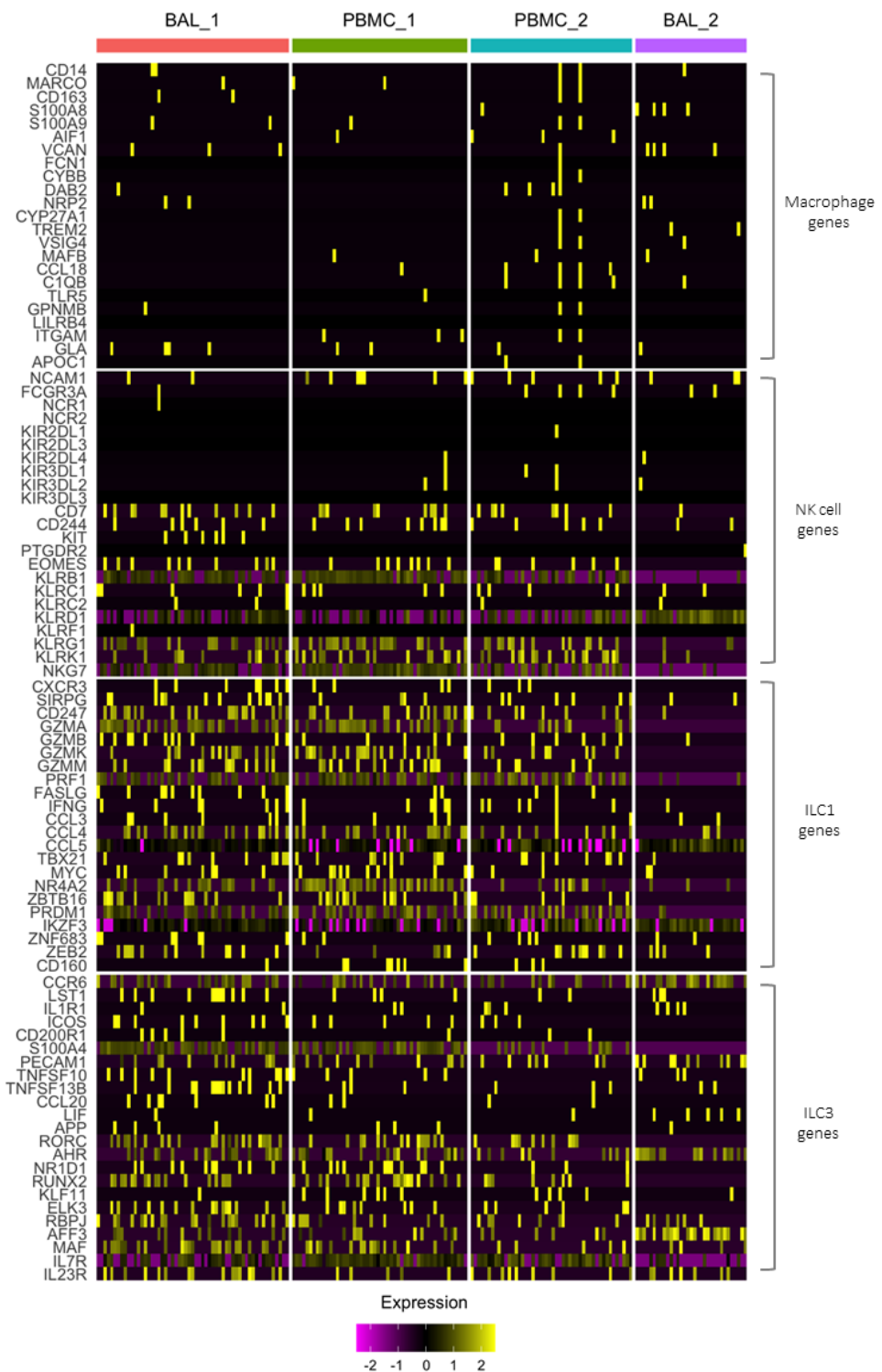
Supplementary Figure 3: Frequency of PD-1 expressing (A) CD8+ MR1 tetramer-positive MAIT cells and (B) CD4-CD8- MR1 tetramer-positive MAIT cells from the peripheral blood of HIV-negative and HIV-positive participants. Bars represent medians and error bars represent interquartile ranges. Statistical difference was determined using the Mann-Whitney *U* test.



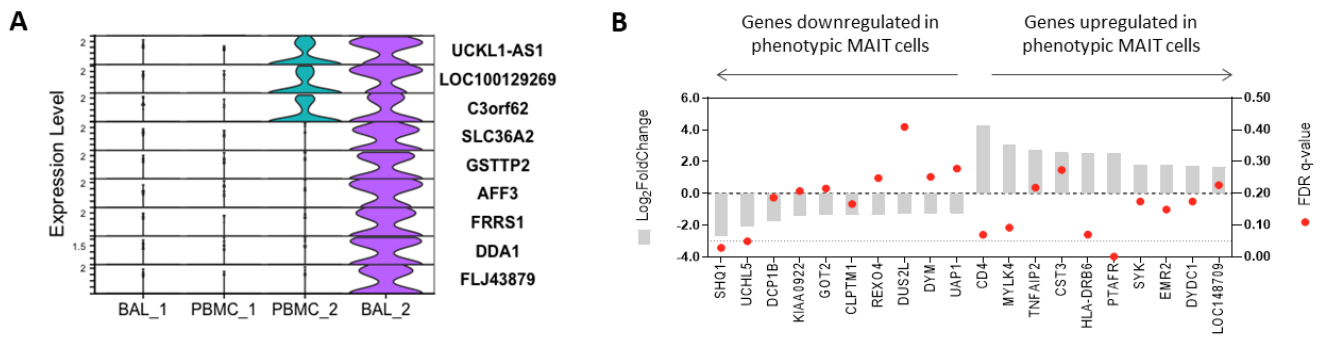
Supplementary Figure 4: (A) Summary of characteristics of MR1 tetramer-positive MAIT cell transcriptomic clusters. (B) UMAP plot showing assignment of HIV status to MAIT cell transcriptomic subsets.



Supplementary Figure 5: Percentage distribution of MAIT cell transcriptomic subsets by each participant identifier (PID) from both the peripheral blood and bronchoalveolar lavage fluid.



Supplementary Figure 6: Heatmap showing the expression of canonical macrophage, natural killer (NK) cell, and group 1 and group 3 innate lymphoid cell (ILC) genes across the four transcriptional MAIT cell subsets.



Supplementary Figure 7: **A)** Violin plot showing the expression of TB-specific TRAV1-2+CD161++CD8+ T cell genes by MAIT cell transcriptional subsets. **B)** Bulk RNA-sequence analysis showing the enrichment of TRAV1-2+CD161++CD8+ T cell genes in bronchoalveolar versus peripheral blood MAIT cells of HIV-negative individuals.